Monitoring Early Breast Cancer Response to Neoadjuvant Therapy Using H-Scan Ultrasound Imaging

Preliminary Preclinical Results

Mawia Khairalseed, PhD, Kulsoom Javed, MD, Gadhvi Jashkaran, BS, Jung-Whan Kim, DVM, PhD, Kevin J Parker, PhD, Kenneth Hoyt, PhD, MBA

Objective—H-scan imaging is a new ultrasound technique used to visualize the relative size of acoustic scatterers. The purpose of this study was to evaluate the use of H-scan ultrasound imaging for monitoring early tumor response to neoadjuvant treatment using a preclinical breast cancer animal model.

Methods—Real-time H-scan ultrasound imaging was implemented on a programmable ultrasound scanner (Vantage 256; Verasonics Inc., Kirkland, WA) equipped with an L11-4v transducer. Bioluminescence and H-scan ultrasound was used to image luciferase-positive breast cancer–bearing mice at baseline and at 24, 48, and 168 hours after administration of a single dose of neoadjuvant (paclitaxel) or sham treatment. Animals were euthanized at 48 or 168 hours, and tumors underwent histologic processing to identify cancer cell proliferation and apoptosis.

Results—Baseline H-scan ultrasound images of control and therapy group tumors were comparable, but the latter exhibited significant changes over the 7-day study ($P < .05$). At termination, there was a marked difference between the H-scan ultrasound images of control and treated tumors ($P < .05$). Specifically, H-scan ultrasound images of treated tumors were more blue in hue than images obtained from control tumors. There was a significant linear correlation between the predominance of the blue hue found in the H-scan ultrasound images and intratumoral apoptotic activity ($R^2 > 0.40$, $P < .04$).

Conclusion—Preliminary preclinical results suggest that H-scan ultrasound imaging is a new and promising tissue characterization modality. H-scan ultrasound imaging may provide prognostic value when monitoring early tumor response to neoadjuvant treatment.

Key Words—apoptosis; cancer; H-scan ultrasound; neoadjuvant treatment; ultrasound

Received July 26, 2018, from the Department of Bioengineering (M.K., K.J., K.H.); Department of Biological Sciences, University of Texas at Dallas, Richardson, Texas, USA (G.J., J.W.K); Department of Biomedical Engineering, Sudan University of Science and Technology, Khartoum, Sudan (M.K.); Department of Electrical and Computer Engineering, University of Rochester, Rochester, New York, USA (K.J.P); Department of Radiology, University of Texas Southwestern Medical Center, Dallas, Texas, USA (K.H.). Manuscript accepted for publication July 22, 2018.

Address correspondence to Kenneth Hoyt, PhD, MBA, FAIUM, University of Texas at Dallas, BSB 13.929, 800 W Campbell Rd, Richardson, TX 75080, Ph: (972) 883-4958.

E-mail: kenneth.hoyt@utdallas.edu

doi:10.1002/jum.14806

Neoadjuvant chemotherapy is the standard of care for treatment of locally advanced breast cancer. Application of systemic therapy before surgery benefits patients with improved rates of breast-conserving therapy. It has also been shown that clinical response to neoadjuvant chemotherapy is correlated with pathologic response at surgery. Clinical studies have further demonstrated that an early neoadjuvant response is a

better predictor of the patient's recurrence-free survival than pathologic complete response.[1] These findings can help guide additional therapy after surgery.

Early functional evaluation of neoadjuvant treatments in oncology is of major importance. Clinical assessment, mammography, sonography, and magnetic resonance imaging, are used extensively to determine response. These methods of assessment involve tracking changes in tumor size.[2] However, measurable changes in tumor size may not manifest until after multiple cycles of chemotherapy.[3] In the interim, significant cost and unnecessary patient toxicity may be incurred for ineffective neoadjuvant therapy regimens.

Apoptosis is a unique type of programmed cell death. Characteristic of solid tumors after treatment,[4] this process involves a sequence of intracellular events that systematically dismantle the cell. The first observable change in a cancer cell undergoing apoptosis is physical shrinkage.[5,6] Drug resistance often prevents cancer cells from undergoing sufficient levels of apoptosis, resulting in cell survival and treatment failure.[7] Collectively, detecting apoptotic events after drug dosing may introduce a new prognostic biomarker for evaluating early treatment response.

Recently, a new tissue characterization modality has emerged for the ultrasound classification of acoustic scatterers.[8–13] Termed H-scan ultrasound (where the *H* stands for hue or Hermite), this imaging approach links a special class of mathematical functions to the physics of ultrasound scattering and reflection from different tissue structures. In practice, digital filters are used to selectively analyze the spectral content of ultrasound backscattered echo signals and to colorize the display, providing visual or quantitative assessment of the major tissue scattering classes. In general, low-frequency spectral content is generated from larger scattering structures and is assigned to red hue, whereas high-frequency echo content is produced by an ultrasound wave interacting with smaller structures of scale below the wavelength of the ultrasound transmit pulse. The high-frequency signals are assigned to blue hue. In short, H-scan sonography may allow clinicians to distinguish subtle cellular and parenchymal changes that would otherwise appear similar on B-scan,[10] thereby adding new information to diagnostic ultrasound imaging.

Materials and Methods

Test Phantom Production

Ultrasound test phantoms were used to test H-scan ultrasound imaging. These phantom materials were homogeneous, containing different-sized scatterers. In short, materials were prepared by heating 10% gelatin (300 Bloom; Sigma Aldrich, St. Louis, MO) in degassed water to 45°C.[14] Silica microspheres that were either 15 or 40 μm in diameter (0.4% concentration; US Silica, Pacific, MO) were introduced during constant stirring. Heated solutions were transferred to rigid molds and placed in a 4°C refrigerator to cool overnight.

Animal Preparation and Study Protocol

Animal experiments were reviewed and approved by our Institutional Animal Care and Use Committee (IACUC). in vivo H-scan ultrasound imaging studies were performed in tumor-bearing animals (N = 25). Luciferase-positive human breast cancer cells (MDA-MB-231; Cell Biolabs, San Diego, CA) were maintained in Leibovitz's L-15 medium supplemented with 10% fetal bovine serum. All cells were cultured to 90% confluence before passaging and grown at 37°C (Heracell 150i, Thermo Fisher Scientific, Waltham, MA). Cell numbers were determined using a digital cell counting instrument (Countess II Automated Cell Counter; Thermo Fisher Scientific, Weaverville, NC). Four-week-old female nude athymic mice (Charles River Laboratories, Wilmington, MA) were implanted orthotopically with 1 million breast cancer cells and allowed to grow until they were about 5 mm in diameter (largest tumor cross section; range, 4–6 weeks).

During the in vivo ultrasound imaging study, animals were placed on a heating pad and controlled with 2% isoflurane anesthesia (mobile anesthesia machine; Parkland Scientific, Coral Springs, FL). Each tumor-bearing animal was sonographically imaged at baseline and before receiving a single injection of paclitaxel (N = 15, 25 mg/kg; Abraxane, Celgene Corp, Summit, NJ) or a matched dose of sham treatment (N = 10, saline) via a tail vein catheter. Terminal end points were either 48 or 168 hours after drug dosing.

In Vivo Small Animal Imaging

Raw radio frequency data was acquired using a Vantage 256 programmable ultrasound research scanner equipped with an L11-4v linear array transducer

Figure 1. Schematic diagram of a first-generation real-time B-scan and H-scan ultrasound (US) imaging system. This clinically translatable and programmable system incorporates a (**A**) graphic user interface for controlling radio frequency data acquisition and signal processing including (**B**) variable control of the parallel convolution filters used to derive the H-scan ultrasound image. System-level data flowchart (**C**) details ultrasound image reconstruction and dual (**D**) H-scan (left) and B-scan (right) display.

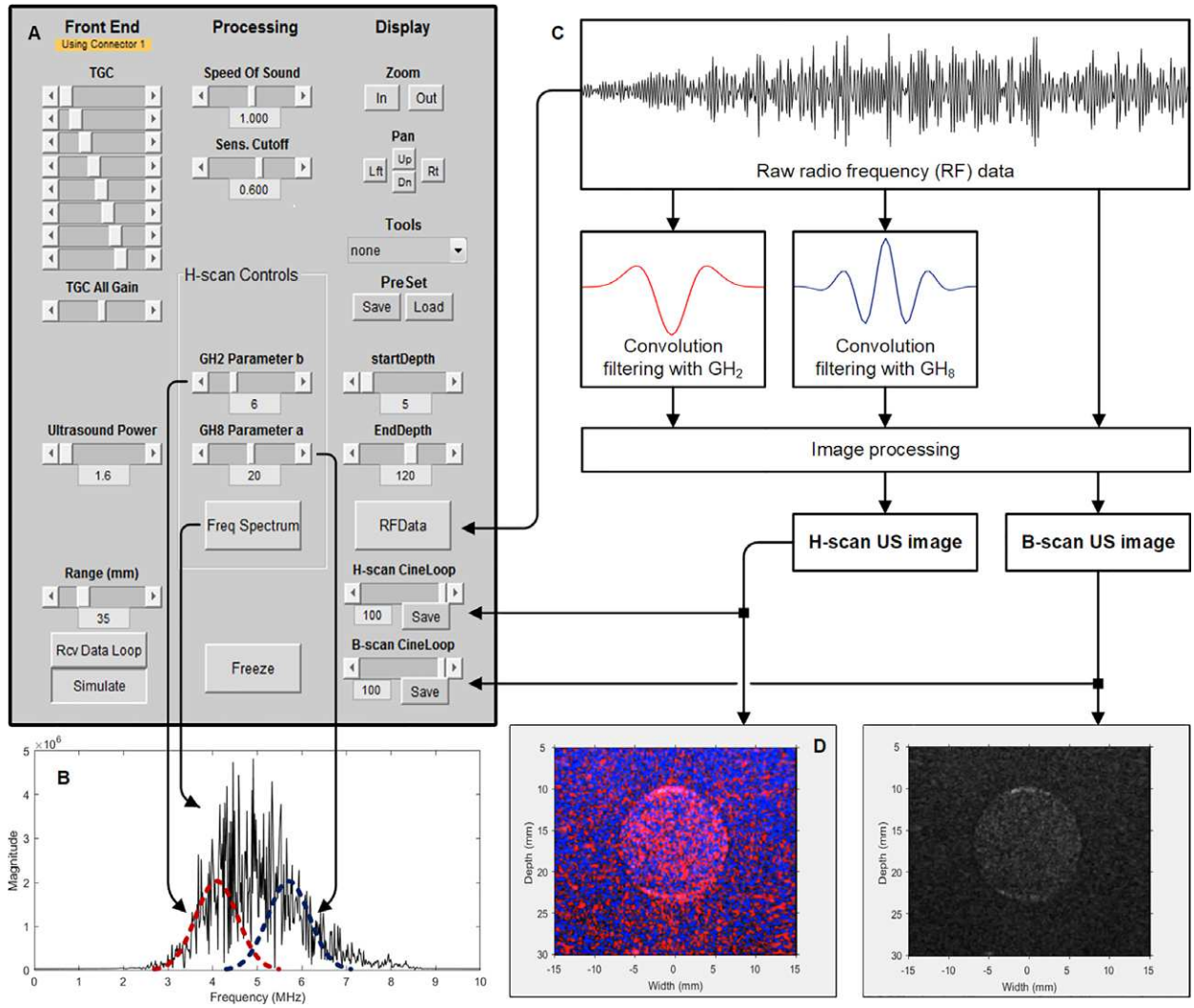

(Verasonics Inc, Kirkland, WA). Ultrafast plane wave imaging was performed using a 5-MHz transmit pulse cycle. Spatial angular compounding was used to improve image quality whereby successively steered and overlapping plane wave transmissions were performed using 5 equally spaced angles in the ±18° range.[10] An acoustic output of 1.1 MPa was employed and measured using a hydrophone scanning system (AIMS III; Onda Corp, Sunnyvale, CA).

Two parallel convolution filters were applied to the radio frequency data sequences to measure the relative strength of the received time-domain signals relative to a pair of Gaussian-weighted Hermite polynomial functions of orders 2 and 8, denoted $GH_2\ (t)$ and $GH_8(t)$, respectively.[8] For each image spatial location, spatial angular compounding was performed by averaging the acquisitions over all steered plane wave transmissions. The signal envelope for each of these filtered and compounded data sequences were then calculated using a Hilbert transformation. The relative strength of these filter outputs is color coded whereby the lower frequency (GH_2) backscatter

signals was assigned to the R channel and the higher frequency (GH_8) components to the B channel. The envelope of the original unfiltered compounded data set is assigned to the G channel to complete the RGB color map and the H-scan ultrasound display image. A schematic diagram summarizing the parallel processing and display of the H-scan ultrasound image is depicted in Figure 1.

Each luciferase-positive tumor-bearing animal was sonographically imaged at baseline and at 24, 48, and 168 hours (ie, 7 days when applicable) after paclitaxel or sham drug dosing. Additionally, optical imaging was performed using a small animal system (Pearl Trilogy; LI-COR Biotechnology, Lincoln, NE) for analysis of cancer cell viability. Tumor areas were manually segmented from the H-scan ultrasound and optical images and the mean signal from each region of interest recorded.

Histologic Processing of Tumor Tissue

Following the last imaging session, animals were humanely euthanized via cervical dislocation. Each animal was then perfused with phosphate-buffered saline and 10 mM of edetic acid followed by 4% paraformaldehyde. Tumor tissue was removed and further fixed in 4% paraformaldehyde overnight followed by paraffin embedding. Tissue sections were stained with hematoxylin and eosin in accordance with standard methods. For immunohistochemistry, 4 different tissue sections (5 μm) from each tumor sample underwent heat-mediated antigen retrieval (citrate buffer, pH = 6). Primary antibodies were applied and incubated at 4°C overnight.[15] The primary antibodies used were cleaved caspase-3 (CC3) and Ki67 (Cell Signaling Technology, Danvers, MA). Digital microscopy images were quantified with ImageJ software.[16]

Statistical Analysis

All group data were summarized as mean ± standard error of the mean. A Mann-Whitney *U* test was used to compare control and therapy measurements. A repeated-measures analysis of variance test evaluated longitudinally collected optical and ultrasound imaging data. A Pearson's correlation test analyzed relationships between imaging and histologic findings at termination. A *P* value less than .05 was statistically significant. All analyses were performed using R software.[17]

Figure 2. B-scan (top row) and H-scan (bottom row) ultrasound images from a tissue-mimicking phantom material containing a homogeneous mixture of (column A) 15-μm or (column B) 40-μm scatterers. Scale bar = 5 mm. Note the increase in H-scan ultrasound image-depicted scatterer size (ie, red hue shift), which is not apparent from inspection of the matched B-scan ultrasound images.

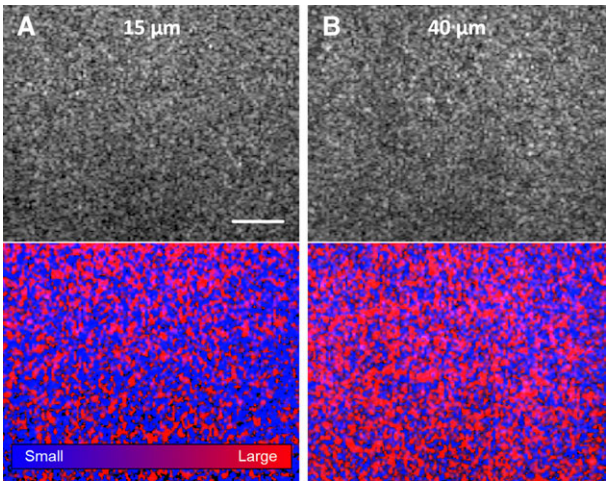

Results

Two different homogeneous phantom blocks were first used to evaluate real-time H-scan ultrasound imaging and its ability to detect relatively small (15 μm) or large (40 μm) acoustic scatterers (Figure 2). Note that each ultrasound image is displayed using an 8-bit dynamic range. While there are no discernible visual differences in the B-scan ultrasound images, review of the H-scan ultrasound images reveals predominant blue intensities from the phantom material composed of smaller spherical scatterers and more red intensities from that containing the larger scatterers. These in vitro results are consistent with the theoretical expectations and serve to verify the H-scan ultrasound imaging technology.

Next, we studied a series of 5 homogenous phantom materials that contained a mixture of both the 15 and 40 μm spherical scatterers of concentrations ranging from 0% to 100%. Representative H-scan ultrasound images of these phantoms are depicted in Figure 3. Also provided is a bar graph summarizing the average blue and red channel amplitudes from each of the H-scan ultrasound images. Inspection of the H-scan ultrasound results does reveal a subtle red to blue shift in image

Figure 3. H-scan ultrasound images from a series of tissue-mimicking phantom materials containing a homogeneous mixture of 2 different microparticles, namely, (**A**) 100% of 40-μm scatterers, (**B**) 75% of 40-μm and 25% of 15-μm scatterers, (**C**) 50% of 40-μm and 50% of 15-μm scatterers, (**D**) 25% of 40-μm and 75% of 15-μm scatterers, and (**E**) 100% of 15-μm scatterers. Scale bar = 5 mm. **F**, Spatial analysis of the red and blue channel signals used to create the H-scan ultrasound images (denoting the relative size of small and large ultrasound scatterers, respectively) reveals that this new tissue characterization technique can detect subtle changes in the distribution of scatterer sizes.

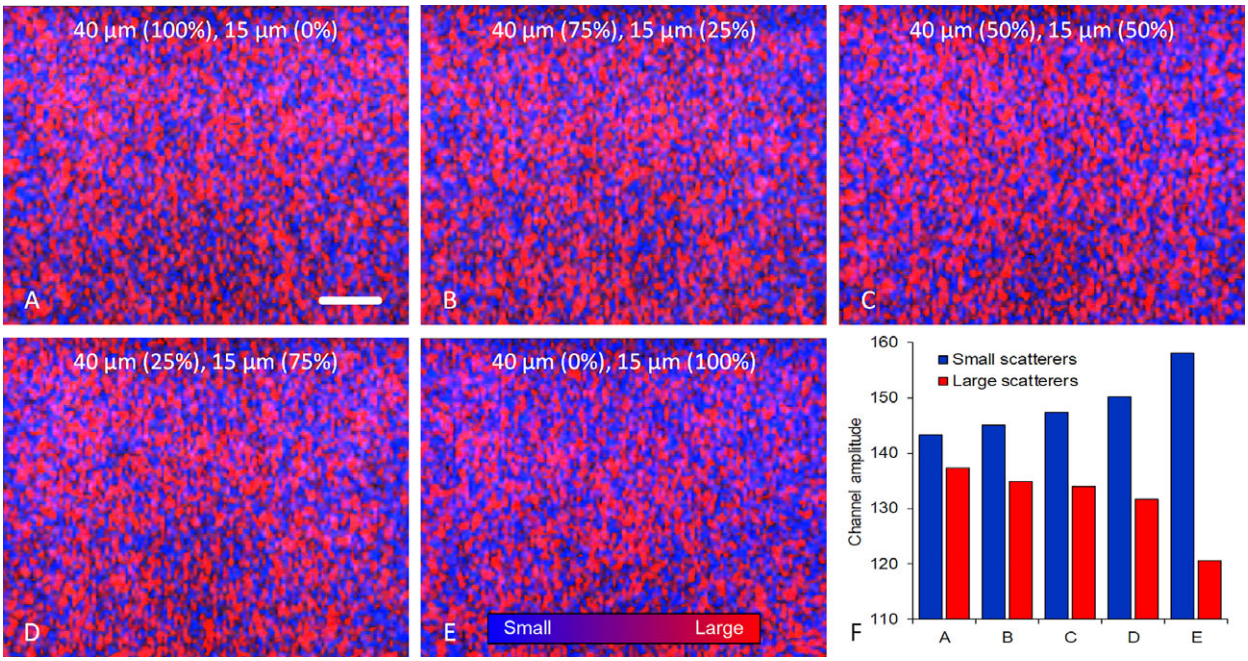

intensity. This trend is much more pronounced from the bar graph data, which clearly highlights the ability of H-scan US to detect relative changes in scatterer size and concentration.

For the in vivo study, there was no difference between control and therapy group tumor sizes at baseline (297 ± 52.4 mm^3 and 212.5 ± 17.5 mm^3, respectively; $P = .31$). Breast cancer–bearing animals were imaged using both bioluminescence and H-scan sonography before and after administration of a single cycle of neoadjuvant treatment with paclitaxel. Figure 4 contains representative images collected at baseline and after dosing with the anticancer drug or sham therapy. Whole animal optical images from control and therapy group tumors exhibit pronounced bioluminescence signal increases, which is reflective of tumor growth and corresponding increases in the overall number of viable luciferase-positive cancer cells. Conversely, while there are no apparent changes in the control H-scan ultrasound images, there does appear to be a discernible temporal shift toward increasing blue intensities for the H-scan ultrasound images obtained from the treated tumor tissue.

A summary of the optical and H-scan ultrasound group data is detailed in Figure 5. Repeated optical measures significantly increased throughout the 7-day study period for both control and therapy group animals ($P < .01$). On the other hand, while there were no temporal changes in the H-scan ultrasound image measures from control animals ($P = .86$), there was a significant 7-day decrease in the mean H-scan image intensity for the treatment group animals ($P = .007$). Noteworthy, the difference between control and therapy group measurements was more pronounced for the H-scan ultrasound images compared to bioluminescence measures of cancer cell viability. Analysis of the individual blue and red channel data used to form the final H-scan ultrasound display images revealed no marked changes in either for the control group data ($P > .29$), but significant increases were found in the blue channel data from treated animals ($P = .045$) and increases that trended toward significance in the red

Figure 4. Representative in vivo (columns **A** and **B**) bioluminescence and (columns **C** and **B**) H-scan ultrasound images of luciferase-positive breast tumor–bearing mice acquired at baseline (0 hours) and again at 24, 48, and 168 hours after receiving a single systemic dose of (columns **A** and **C**) sham treatment or (columns **B** and **D**) neoadjuvant chemotherapy.

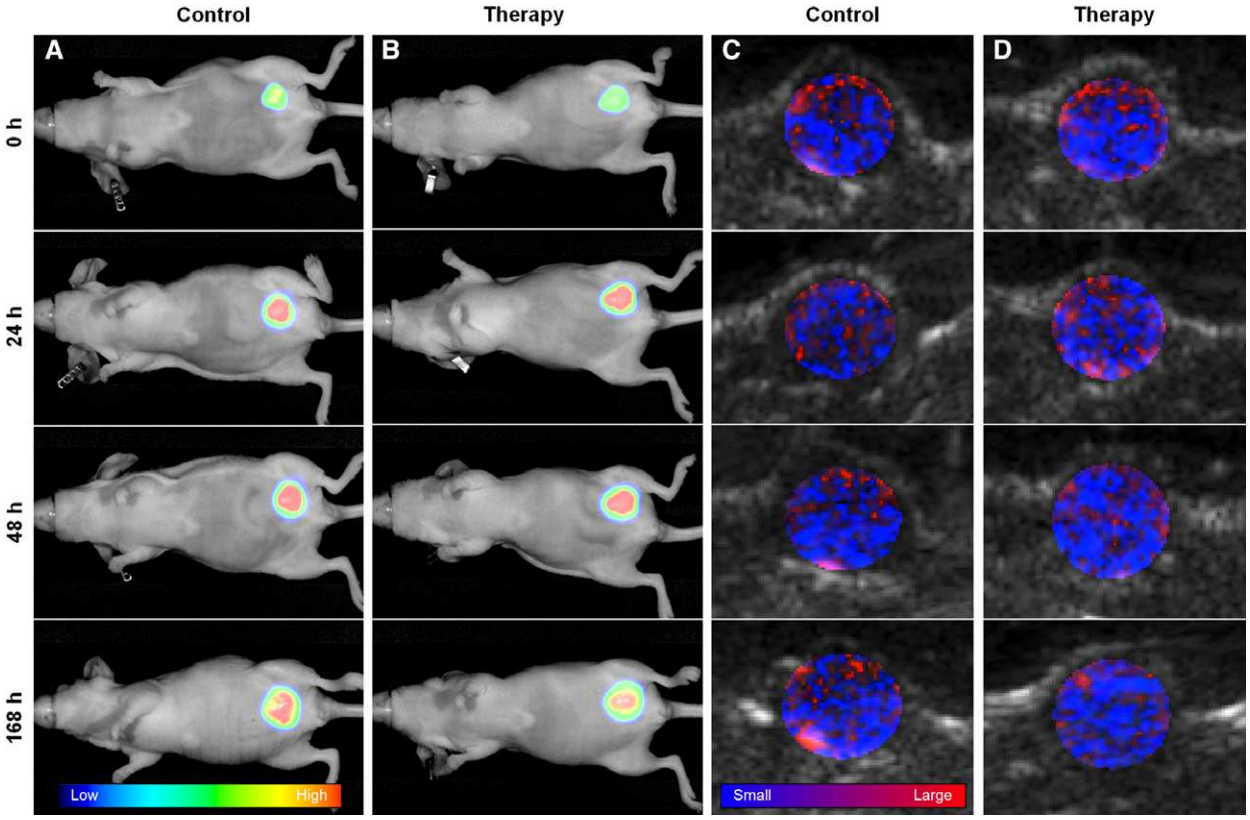

channel data ($P = .06$). A comparison between control and treated animal group measurements collected on the same experimental day revealed significant differences at 7 days for the H-scan ultrasound data ($P = .04$), at 48 hours and 7 days for the blue channel data ($P < .02$), and at baseline for the red channel data ($P = .03$). Further analysis of blue and red channel data versus tumor size at baseline discovered no notable relationship for the former ($R^2 = 0.02$, $P = .53$) and a significant positive correlation for the latter ($R^2 = .43$, $P < .001$). Given that the tumor sizes in the control group were larger at baseline compared to the treatment group animals, this may explain in part the difference in red channel measurements before neoadjuvant chemotherapy was administered.

All animals were terminated either at 48 hours or 7 days after administration of a single cycle of neoadjuvant treatment. By 7 days, tumor growth was considerably retarded in the treated animals (442.2 ± 70.3 mm^3) compared to the controls (867.5 ± 278.8 mm^3). Improper tissue sectioning or staining resulted in 4 samples being excluded from further analysis. Representative histologic images from processed tumor tissue samples are illustrated in Figure 6. For both control and treated tumor sections, there was pronounced cancer cell proliferation and discrete apoptotic activity at both terminal time points. A comparison of the control and therapy group histologic findings found no significant differences in either the extent of cancer cell proliferation (Ki67, $P > .20$) or apoptotic activity (caspase-3, $P = .22$). While apoptotic activity was noticeably reduced 7 days after drug dosing, it was more pronounced for the therapy tumor group.

A final correlation analysis between ultrasound-based image and tumor histologic measures at

Figure 5. Summary of longitudinal control and therapy group (**A**) bioluminescence, (**B**) H-scan ultrasound, (**C**) blue channel amplitude, and (**D**) red channel amplitude (eg, used in part to construct the H-scan ultrasound image) measurements. Asterisk indicates $P < .05$ versus control data.

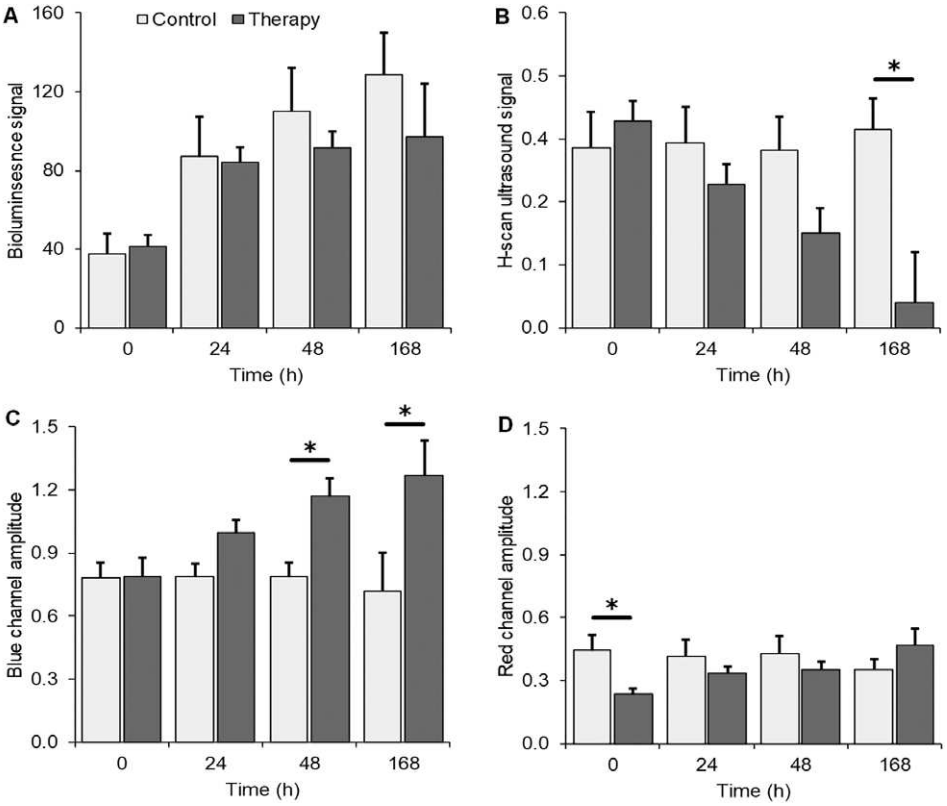

termination was performed, and the results are shown in Figure 7. Analysis of cancer cell proliferation scores versus ultrasound imaging results revealed no significant trends ($P > .23$). Conversely, and of note from the therapy group findings, there were statistically significant relationships between both H-scan sonography or blue channel data and intratumoral apoptotic activity ($R^2 = 0.50$, $P = .01$ and $R^2 = 0.40$, $P = .04$, respectively) that was not found with the control measurements ($P = .49$).

Discussion

The real-time H-scan analysis of ultrasound images is a match-filter approach derived from analysis of scattering from incident pulses in the form of Gaussian-weighted Hermite polynomial functions. Tissue-mimicking phantom materials were used to verify the utility of H-scan ultrasound imaging and demonstrate a capability of differentiating scattering objects by size. A homogenous phantom containing 15 μm spherical scatterers produced H-scan ultrasound images that were predominantly blue in color, while the phantom made using the larger 40-μm scatterers resulted in more red hue in the H-scan ultrasound images. After introducing both different-sized scatterers into a series of different phantom materials, H-scan ultrasound imaging successfully identified changes in scatterer concentration. More specifically, phantoms containing a higher concentration of the 15 μm spherical scatterers produced H-scan ultrasound images that had more blue hue compared to the phantoms containing more of the 40-μm scatterers, which yielded H-scan ultrasound images that were more red. Collectively, these findings are in agreement with the theoretical foundation of relative scatterer size estimation using H-scan ultrasound imaging.[8]

Figure 6. Representative histology stains for (**A**) Ki 67 (cell proliferation, black arrows) and (**B**) caspase-3 (cell apoptosis, black arrows) of tissue sections from control and treated tumors. Group measurements are summarized for (**C**) tumor size, (**D**) Ki 67, and (**E**) caspase-3 at animal termination.

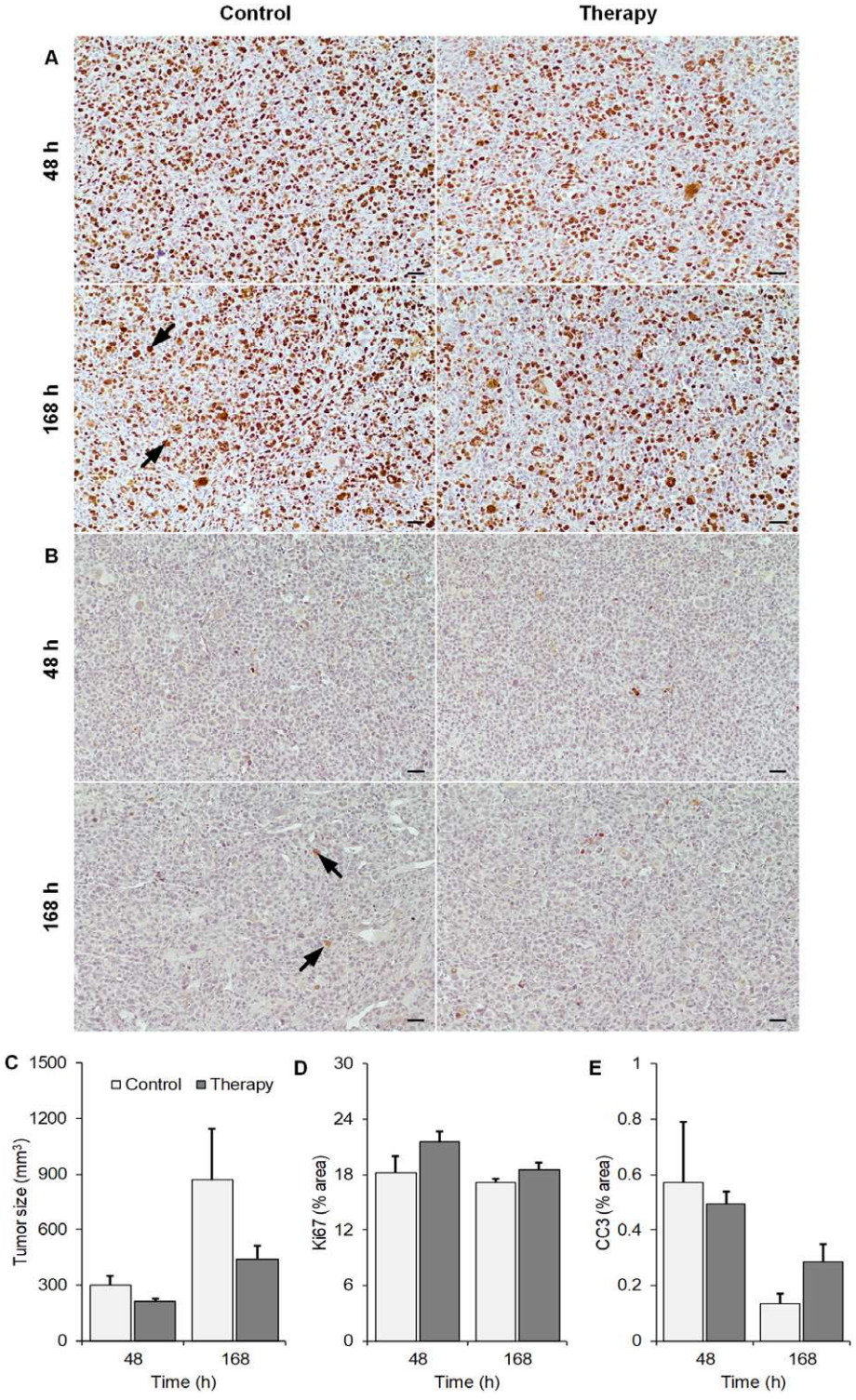

Figure 7. Scatter plot data from treated tumors of mean (**A, D**) H-scan ultrasound, (**B, E**) blue channel amplitude, and (**C, F**) red channel amplitude plotted as a function of cell proliferation (Ki67, top) or apoptotic activity (caspase-3, bottom). Regression analysis reflects presence of any linear relationships.

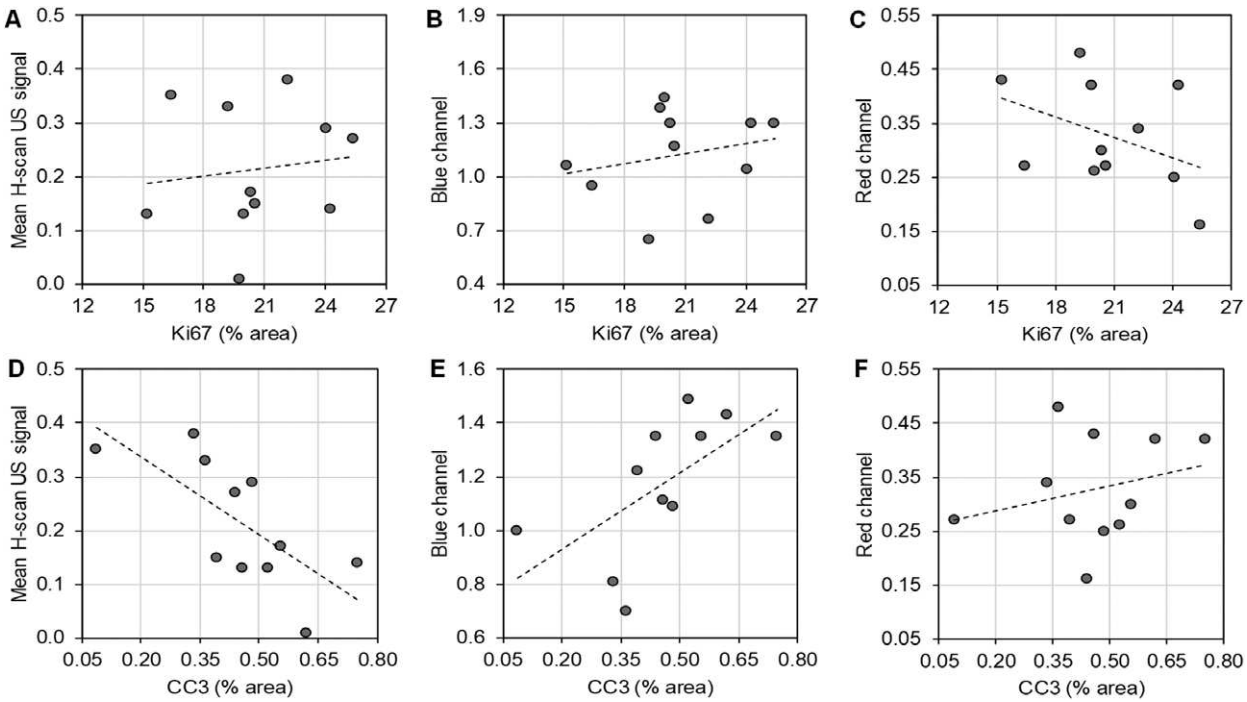

Using a luciferase-positive breast cancer xenograft model, H-scan ultrasound was used to image the developed tumors following administration of a single session of neoadjuvant chemotherapy (ie, paclitaxel) versus sham treatment. Both in vivo H-scan ultrasound imaging bioluminescence imaging was performed at baseline and again at 24, 48, and 168 hours (7 days when applicable). Animals were humanely euthanized at either 48 or 168 hours to allow for histologic processing of excised tumor tissue. As a general observation, larger tumors tended to exhibit an H-scan ultrasound reddish pattern around the tumor periphery, which may be attributed to increased extracellular matrix density.[18] While baseline H-scan ultrasound images of control and therapy group tumors were comparable, the latter exhibited significant changes throughout the 7-day study ($P < .05$). At termination there were, on average, marked differences between the H-scan ultrasound images of the control and the therapy group tumors ($P < .05$), which were more pronounced than those found using bioluminescence imaging of cancer cell viability. More specifically, H-scan ultrasound images of the treated tumors were more blue in hue than images obtained from the control tumor tissue. It is worth noting that there was a significant linear correlation between the predominance of the blue hue found in the H-scan ultrasound images and mean intratumoral apoptotic activity ($R^2 > 0.40$, $P < .04$) in animals administered a single dose of chemotherapy. Given that paclitaxel is a class of chemotherapeutics that inhibits cellular mitosis leading to apoptosis, we theorize that the progressive color map shift observed in the longitudinal H-scan ultrasound images is, in fact, detection of cancer cell shrinkage in the whole tumor mass as the cells undergo apoptotic death.[5,6]

One limitation of this study involves a lack of physical measurements of the different ultrasound scattering objects in the cancerous tissue, which future work could address and directly estimate from pathology slides.[19] This approach would help validate the in vivo H-scan ultrasound findings and for

improved modeling of ultrasound scattering from breast abnormalities. A technological limitation of this study is that no modifications were made to the ultrasound transmit pulse excitation to improve conformity to a Gaussian-weighted Hermite polynomial. Given that the real-time H-scan ultrasound imaging approach used for this study was implemented using a programmable ultrasound research scanner, future work should implement this new pulse sequence to improve the H-scan analysis of the different tumor tissue scatterers.

Conclusion

Real-time H-scan is a new ultrasound-based imaging technique that locally estimates the relative size and spatial distribution of ultrasound scattering objects and structures. Preliminary results using an animal model of breast cancer suggests that in vivo H-scan ultrasound imaging is a promising tissue characterization modality. Furthermore, H-scan ultrasound imaging may provide prognostic value when monitoring the early tumor response to neoadjuvant treatment and more research is warranted.

References

1. Hylton NM, Gatsonis CA, Rosen MA, Lehman CD, Newitt DC, Partridge SC, et al. Neoadjuvant chemotherapy for breast cancer: functional tumor volume by MR imaging predicts recurrence-free survival-results from the ACRIN 6657/CALGB 150007 I-SPY 1 TRIAL. *Radiology* 2016; 279:44–55.
2. Eisenhauer EA, Therasse P, Bogaerts J, et al. New response evaluation criteria in solid tumours: revised RECIST guideline. *Eur J Cancer* 2009; 45:228–247.
3. Brindle K. New approaches for imaging tumour responses to treatment. *Nat Rev Cancer* 2008;8:94–107.
4. Mesner PW, Budihardjo II, Kaufmann SH. Chemotherapy-induced apoptosis. *Adv Pharmacol* 1997; 41:461–499.
5. Tengku Din TADA-A, Seeni A, Khairi W-NM, Shamsuddin S, Jaafar H. Effects of rapamycin on cell apoptosis in MCF-7 human breast cancer cells. *Asian Pac J Cancer* 2014; 15: 10659–10663.
6. Shen H, Zhao S, Xu Z, Zhu L, Han Y, Ye J. Evodiamine inhibits proliferation and induces apoptosis in gastric cancer cells. *Oncol Lett* 2015; 10:367–371.
7. Wilson TR, Johnston PG, Longley DB. Anti-apoptotic mechanisms of drug resistance in cancer. *Curr Cancer Drug Targets* 2009; 9:307–319.
8. Parker KJ. Scattering and reflection identification in H-scan images. *Phys Med Biol* 2016; 61:L20–L28.
9. Khairalseed M, Xiong F, Mattrey RF, Parker KJ, Hoyt K. Detection of early tumor response to Abraxane using H-scan imaging: preliminary results in a small animal model of breast cancer. *Proc IEEE Ultrason Symp* 2017:1–4.
10. Khairalseed M, Xiong F, Kim J-W, Mattrey RF, Parker KJ, Hoyt K. Spatial angular compounding technique for H-scan ultrasound imaging. *Ultrasound Med Biol* 2018; 44:267–277.
11. Khairalseed M, Hoyt K, Ormachea J, Terrazas A, Parker KJ. H-scan sensitivity to scattering size. *J Med Imaging* 2017; 4: 043501.
12. Parker KJ. The H-scan format for classification of ultrasound scattering. *OMICS J Radiol* 2016; 5:236.
13. Ge GR, Laimes R, Pinto J, et al. H-scan analysis of thyroid lesions. *J Med Imaging* 2018; 5:013505.
14. Hoyt K, Kneezel T, Castaneda B, Parker KJ. Quantitative sonoelastography for the in vivo assessment of skeletal muscle viscoelasticity. *Phys Med Biol* 2008; 53:4063–4080.
15. Goodwin J, Neugent ML, Lee SY, Choe JH, Choi H, Jenkins DMR, et al. The distinct metabolic phenotype of lung squamous cell carcinoma defines selective vulnerability to glycolytic inhibition. *Nat Commun* 2017; 8:15503.
16. Schneider CA, Rasband WS, Eliceiri KW. NIH Image to ImageJ: 25 years of image analysis. *Nat Methods* 2012; 9:671–675.
17. R Core Team. *R: A language and environment for statistical computing [Internet]*. Vienna, Austria: R Foundation for Statistical Computing. http://www.R-project.org/. Published 2016. Data accessed 03/15/2018
18. Venning FA, Wullkopf L, Erler JT. Targeting ECM disrupts cancer progression. *Front Oncol* 2015; 5:224.
19. Waag RC. A review of tissue characterization from ultrasonic scattering. *IEEE Trans Biomed Eng* 1984; 31:884–893.